Published in final edited form as:

Nat Neurosci. 2009 June ; 12(6): 745–750. doi:10.1038/nn.2313.

Na^+-activated K^+ channels express a large delayed outward current in neurons during normal physiology

Gonzalo Budelli[1,2], **Travis A. Hage**[1,2], **Aguan Wei**[1,3], **Patricio Rojas**[1], **Ivy Yuh-Jiin Jong**[1], **Karen O'Malley**[1], and **Lawrence Salkoff**[1,4]

[1]Department of Anatomy and Neurobiology, Washington University School of Medicine, 660 S. Euclid Avenue, Saint Louis MO, 63110

[4]Department of Genetics, Washington University School of Medicine, 660 S. Euclid Avenue, Saint Louis MO, 63110

Abstract

One of the largest components of the delayed outward current active during normal physiology in many mammalian neurons such as medium spiny neurons of the striatum and tufted–mitral cells of the olfactory bulb, has gone unnoticed and is due to a Na^+-activated-K^+-current. Previous studies of K^+ currents in mammalian neurons may have overlooked this large outward component because the sodium channel blocker tetrodotoxin (TTX) is typically used in such studies; we find that TTX also eliminates this delayed outward component as a secondary consequence. Unexpectedly we found that the activity of a persistent inward sodium current (persistent I_{Na}) is highly effective in activating this large Na^+-dependent (TTX-sensitive) delayed outward current. Using siRNA techniques we identified SLO2.2 (Slack) channels as carriers of this delayed outward current. These findings have far reaching implications for many aspects of cellular and systems neuroscience, as well as clinical neurology and pharmacology.

The original discovery of high conductance sodium-activated potassium channels (K_{Na} channels) in heart (1) and brain (2,3) presented a conundrum; studies of single channel properties in inside-out patches showed that they respond to very high levels of Na^+, far exceeding that present in the normal intracellular bulk cytosol (1–5). Hence, it was suggested that this channel class represents a reserve conductance to be activated during times of stress due to ischemia or hypoxia, when sodium ion accumulates in cells (1,6). However, other studies indicated that K_{Na} channels may be active under normal physiological conditions (6–9), but the effectiveness of sodium entry through voltage-

Corresponding author: Lawrence Salkoff. Department of Anatomy and Neurobiology, Washington University School of Medicine, 660 S. Euclid Avenue, Saint Louis MO, 63110, Phone (314) 362-3644. Fax: (314) 362-3446. Email: SalkoffL@pcg.wustL.edu.

[3]Current address Center for Neuroscience, Seattle Children's Research Institute, M/S C9S-8, 1900 9th Ave. Seattle, WA 98101

[2]Authors contributed equally to this work

Author contributions

G.B. and T.H. undertook the major electrophysiological experiments and analysis of MSNs and Tufted-Mitral cells; A.W. and P.R. aided these studies and undertook control experiments; Y-J I.J. and K.O'M. conducted immunocytochemical studies and Western blotting experiments, and also supported dissections and preparation of cell cultures; L.S. designed and supervised the study and wrote the paper, all in close consultation with GB and TH.

dependent sodium channels in activating K_{Na} channels remained in dispute (4,7). To explore these questions we undertook a study of the action of the sodium channel blocker tetrodotoxin (TTX) on outward currents in several types of rat neurons. We discovered that many neuronal cell types have a TTX-sensitive delayed outward current that decays only slightly over the time course of a second.

To demonstrate the effectiveness of Na^+ entry through TTX-sensitive sodium channels in activating the delayed outward current we adjusted the intracellular concentration of Na^+ to very low levels by removing Na^+ from the intracellular pipette recording solution so that any intracellular Na^+ would be a minor residual. Under these conditions we applied voltage step pulses to voltage clamped neurons and compared the delayed outward current before and after the addition of TTX. Figure 1(a–c) shows the results of such experiments in a tufted/mitral cell (a), a medium spiny neuron of the striatum (MSN) (b), and a cortical pyramidal cell (c). The delayed outward current component was plotted as the average current during the interval of 150 to 250 ms after the initiation of step pulses. Total outward currents are shown before and after the addition of TTX. The difference between the traces represents the TTX-sensitive delayed outward K^+ current. The addition of TTX reduced the delayed outward current in MSNs by 43.3% +/− 2.5% (n=14) P=<0.01, and 57.2% +/− 3.6%, (n=21) P=<0.01 in tufted/mitral cells. In cortical pyramidal cells the reduction was smaller but still represented a significant component in about half of the cells (Fig. 1c). To further validate that the TTX-sensitive outward current was evoked by the influx of sodium, we removed extracellular Na^+ instead of adding TTX, and found that the results of this treatment were similar to the effects of adding TTX, reducing the delayed outward current by 49% (Fig. 2a). The effect of eliminating extracellular Na^+ is readily reversible, although perhaps not totally (Fig. 2a). As an additional method of showing the selective activation of the delayed outward current by Na^+ entry, we substituted equimolar lithium ion (140 mM) for external Na^+. Although Li^+ is carried by voltage-gated sodium channels, prior studies had shown that K_{Na} channels are insensitive to Li^+ (6). Our experiments substituting Li^+ for Na^+ showed that it had a similar effect to TTX, reducing the delayed outward current in MSNs by 41.6% vs. a 43% reduction by TTX (Fig. 2b). This result not only shows the specificity of Na^+ influx for activation of the delayed outward current, but also eliminates the possibility of artifact due to changing space-clamp conditions by TTX addition or Na^+_o removal.

Tufted/mitral cells of the rodent olfactory bulb had been used in classic studies (3, 10) to show the properties of Na^+-activated potassium channels in mammalian neurons because they are abundant in these cell types. Our laboratory had previously shown that the SLO2.2 (Slack) gene encoded a Na^+-activated potassium channel (11), and it was demonstrated by immunocytology and in-situ technique, that Slack channels were expressed in those cell types (12). Hence, the Slack channel gene was a prime candidate to carry the Na^+-dependent delayed outward current that we observed. An immunocytochemical survey of many areas of the rodent brain had shown that the Slack gene was widely expressed in both cortical and subcortical regions (12). However, in contrast to the olfactory bulb cells, Slack channel expression in MSNs had not been well studied, but as shown, we had detected that a substantial fraction of the delayed outward current was Na^+-dependent. Thus, we sought to verify that Slack channels were expressed in MSNs and that Slack channels carried the large

Na^+-dependent delayed outward current in those cells. We positively identified Slack channel expression in MSNs using a variety of techniques including Western Blots and rtPCR (Supplementary Figure 1). The expression of Slack channels in MSNs was also independently verified in another laboratory by *in situ* hybridization (13). To investigate whether Slack channels actually carried the Na^+-dependent delayed outward current in MSNs we designed siRNA primers to knock down Slack expression in these cells, with the expectation that Slack-siRNA treatment would remove or reduce the Na^+-dependent outward current present in MSNs. siRNA design was based on Pei and Tuschl (14). Supplementary Figure 2 shows control experiments on a HEK cell line stably transfected with the *Slack* gene. In these experiments we showed the efficient knockdown of Slack channel expression by anti-Slack siRNA monitored by both immunocytological staining (supp Fig. 2b) and physiological recordings (supp Fig. 2c). We then used the siRNAs validated by these experiments to knock down Slack current expression in primary cell cultures of MSNs (Fig. 1e). In MSNs transfected with Slack-siRNA (and a GFP-expressing vector) TTX reduced the delayed outward current by only 16.8 % +/− 3.2% (n=8) while in MSNs transfected with a control siRNA (Slick) (and a GFP-expressing vector), TTX reduced the current 34.0% +/− 3.9% (n=8) P=<0.01.

A persistent Na^+ current activates Na^+-dependent delayed outward current

One indicator was that the sodium-dependent delayed outward current persisted long after the transient sodium current was fully inactivated. Indeed, the sodium-dependent delayed outward current showed only a minor decay even during step pulses lasting for 1000 ms (Fig. 1b). We showed the importance of the persistent I_{Na} component relative to the transient I_{Na} component in activating the sodium-dependent delayed outward current, using two separate methods. The first method employed the pharmacological agent Riluzole which preferentially blocks the persistent I_{Na}, over the transient component of the sodium current (15). Riluzole is known to block the persistent sodium current by stabilizing the inactivated state of the sodium channel, thereby preventing re-openings (flickering) of the channel (15). The effect of Riluzole is shown in Figure 3a–c. In this experiment a large fraction of the delayed outward current is reduced by the application of Riluzole (20 μM) (Fig. 3a), but the transient sodium current is not reduced (Fig. 3b). The plotted data in Figure 3a shows the current-voltage relation for the currents, before and after the application of Riluzole, and current-voltage relation for the subtracted (Riluzole-sensitive) component. Figure 3c shows the base of the curves on an expanded scale. The arrow indicates that the subtracted (Riluzole-sensitive) component also includes a persistent inward current, as well as the delayed outward component. Note that the plotted currents represent average values at 150–250 ms, long after the cessation of the transient inward component. Thus, Riluzole removed the sodium-dependent outward current and the persistent I_{Na}, but not the transient I_{Na}. This shows that the persistent I_{Na+} was the more important inward component coupled to the Na^+-dependent delayed outward component. [Note that control experiments in our stably Slack-transfected-HEK cell line showed no reduction of the Slack delayed outward current by Riluzole (see figure legend 3 for statistics).] In MSNs, Riluzole (20 μM) was slightly less effective than TTX in reducing the delayed outward current, reducing it 30.1% (+/− 3.09%, n=9; p<.01). Thus, since a large fraction of the transient I_{Na} remains after the application of

Riluzole, the transient sodium current does not appear to be the major factor in activating the sodium-dependent delayed outward current.

The second method of showing the importance of the persistent I_{Na} used a relatively depolarized holding potential (−50 mV) to inactivate the transient I_{Na} component. In these experiments the TTX-sensitive delayed outward current is still present as shown by the significant reduction of the delayed outward current after the addition of TTX (Fig. 3d). In Figure 3d the TTX-sensitive outward component is larger than the remaining outward current, and is shown in the bottom traces as the difference between the control current, before TTX, and the remaining current after TTX-application. At a holding potential of .−50 mV persistent sodium currents are active in most neuronal cell types including MSNs (16,17,18). The amplitudes of persistent sodium currents are often only a fraction of peak transient sodium currents, but are active over a broader voltage range (16,17,18). It is now widely accepted that several of the voltage-dependent sodium channel types which carry fast transient Na^+ currents, also carry persistent sodium currents (16,17), but we have not established the genetic identity of the persistent Na^+ currents in the cells we are studying. Both types of experiments shown in Figure 3 indicate that the persistent Na^+ current is the largest factor in activating the Na^+-dependent delayed outward current, but we cannot rule out the transient Na^+-current as a contributing factor.

Experiments to measure the persistent Na^+ current in MSNs (Fig. 4) show a current which is only a small fraction of the peak transient Na^+ current, as had been previously reported (18). Also, as previously reported, we found the persistent Na^+ current to be active over a wider voltage range than the transient Na^+ current, with some current noted at negative potentials of at least .−70 mV. Note that in the experiments plotted in Figure 4d we adjusted the Na^+ equilibrium potential to approximately +23 mV to improve voltage control by raising internal [Na^+] (Fig. legend 4). The lower driving force on Na^+ resulted in a smaller sodium current than would be seen under normal physiological conditions, and showed a reversal potential close to E_{Na}. Experiments raising E_{Na} by lowering internal [Na^+] indicated little inactivation of the persistent I_{Na+} at voltages exceeding +23 mV.

Na^+-activated K^+ channels and Na^+ channels may be tightly clustered

Given the high [Na^+]i requirements for Na^+-activated K^+ channel activation (1,5,11), it seems unusual that such a small Na^+ current could effectively activate these K^+ channels. However, during a depolarizing step pulse, the transient I_{Na+} is only maximal for 1 to 2 ms, whereas the persistent Na^+ current, although smaller, is active indefinitely as long as sufficient depolarization is maintained. It may also be continuously active at or near cell resting potentials, albeit to a smaller degree. Conceivably, both Na^+-activated K^+ channels and sodium channels might be tightly clustered in a microdomain that permitted an increased concentration of Na^+ relative to the bulk cytosol, similar to that seen for Ca^{2+} microdomains where calcium channels and Ca^{2+}-dependent K^+ channels are clustered (19). Considering the high diffusion constant for Na^+, we considered the possibility that a Na^+ microdomain might consist of an “unstirred layer” (20,21) or “fuzzy space” (22,23) that restricted the diffusion of Na^+, but such a space would also restrict the movement of K^+ thus lowering the K^+ conductance of Na^+-activated K^+ channels. However, an alternative

mechanism for the creation of a Na^+-rich microdomain might be an electrostatic environment that concentrates Na^+ at a level higher than the bulk cytoplasm. Such an electrostatic microdomain for enrichiment of K^+ is present at the entrance to the intracellular vestibule of the BK (SLO1) channels which have a ring of eight negatively charged glutamate residues (24,25). This ring of charge was shown to double the conductance of SLO1 channels by increasing the concentration of K^+ in the vestibule through an electrostatic mechanism. Amazingly, the concentration of K^+ in the vestibule by the ring of charge was calculated to be equivalent to that achieved by increasing the K^+ in the bulk intracellular solution from 150 to 500 mM. (24,25). Such a simple electrostatic mechanism might function alone or in conjunction with an "unstirred layer" or "fuzzy space" in order to raise the local concentration of Na^+ to a higher concentration than the bulk cytoplasm.

TTX–sensitive Na^+ entry raises local $[Na^+]_i$ even in Na^+-loaded neurons

We conducted experiments where the internal $[Na^+]$ was raised by filling whole cell patch recording electrodes with intracellular recording solutions containing 20, 30 and 40 mM Na^+. In these experiments, we found that even though $[Na^+]_i$ was elevated, additional Na^+ influx during voltage clamp step pulses produced an incremental increase in the delayed outward current noted as a TTX-sensitive component. This was true even though sodium entry during voltage clamp step pulses was unlikely to appreciably raise the concentration of bulk $[Na^+]_i$. One possibility to explain the effectiveness of continued sodium entry during depolarizing step pulses is that persistent sodium entry in close proximity to Slack channels is the critical factor. We reasoned that if an inward Na^+ current in close vicinity to the Slack channels can raise the local $[Na^+]$ to a higher level than the bulk intracellular solution, then an outward Na^+ current in close proximity to the Slack channels may deplete the local $[Na^+]_i$. Thus, reversing the direction of TTX-sensitive sodium flux across the membrane in these Na^+ loaded cells should result in a local $[Na^+]_i$ which is lower than that achieved simply by blocking outward Na^+ flux with TTX. Figure 5a shows the results of an experiment to test this possibility. To raise $[Na^+]_i$ we filled the intracellular pipette with a solution containing 40 mM Na^+, lowering K^+ by an equal amount. A series of control voltage-clamp step pulses were then applied at 10 mV intervals to a maximum of +90 mV. We next reversed the direction of Na^+ current flow along the entire voltage range by reducing the extracellular $[Na^+]$ to 0. After approximately a minute and a half, we repeated the series of voltage clamp step pulses and observed a substantially diminished delayed outward current. Finally, we added TTX to the extracellular solution containing 0 Na^+ and, after approximately one minute and a half, we again repeated the series of voltage-clamp step pulses. At this final condition, the delayed outward current was larger, relative to the current with 0 mM $[Na^+]_o$. Our interpretation is that in the first series of control voltage clamp step pulses, Na^+ entry raised the $[Na^+]$ in the vicinity of Slack channels to a level higher than that present in the bulk intracellular solution. However, after removing extracellular Na^+, sodium moved in the outward direction across the membrane diluting the intracellular Na^+ in the immediate vicinity of Slack channels to a lower level than would be present if the outward flow of Na^+ was blocked. Finally, after adding TTX to the extracellular solution containing 0 Na^+, the outward flow of Na^+ was reduced and the concentration of Na^+ in the vicinity of Slack channels rose to a level intermediate between

control conditions, when the Na^+ current was inward, and condition 2 when the Na^+ current was outward. Figure 5a also shows the residual delayed outward currents obtained by subtracting the currents recorded after removal of external Na^+, from the control currents recorded in normal $[Na^+]_o$, and the residual currents obtained by subtracting the currents recorded after addition of TTX to 0 mM external Na^+, from the control currents recorded in normal $[Na^+]_o$ (Fig. 5a). Notably, these residual currents decline at higher voltages. This is likely to be due to the fact that Slack channels at higher voltages are particularly vulnerable to block by $[Na^+]_i$ (6,11). This could also be due to the fact that the sodium current was outward at the higher voltage steps for the control currents recorded in normal $[Na^+]_o$ and therefore the outward flow of Na^+ could partially deplete the local concentration of Na^+ sensed by SLO2 channels. However, we have noted that the reduction of outward current after TTX is added (as in Fig. 1a–c) is not immediate and requires approximately 1 to 2 min. before the current is stabilized at the lower level. Thus, the local concentration of Na^+ sensed by SLO2 channels may only be partially changed during shorter voltage clamp step pulses.

Figure 5a clearly suggests that, even if the internal bulk concentration of Na^+ is raised to as high as 40 mM, there appears to be an additional rise in the Na^+ concentration in the vicinity of Slack channels during depolarizing step pulses, as long as the driving force on Na^+ is inward. To explore this further, we conducted a series of experiments on cells “loaded” with different intracellular concentrations of Na^+ and subjected to a series of voltage clamp step pulses. The object was to examine the incremental rise in the Na^+-dependent delayed outward conductance due to Slack channel activation by Na^+ influx augmenting the level of Na^+ already present in the presumed microdomain. These experiments are shown in Figure 5b where conductance-voltage relations show the normalized incremental conductance increases in the Na^+-dependent delayed outward current due to Na^+ crossing the membrane from cells with different levels of $[Na^+]_i$. These incremental conductance-voltage curves were constructed from the residual currents obtained by subtracting the currents recorded after removal of external Na^+, from the control currents recorded in normal $[Na^+]_o$ (as in Figure 5a, subtraction 1–2). An examination of the incremental conductance curves plotted in Figure 5b for 0, 20, and 30 mM $[Na^+]_i$ show two significant features; as $[Na^+]_i$ increases, the curves shift leftward to more negative voltages, and also show a steeper slope. This seems consistent with the hypothesis that, at higher concentrations of bulk $[Na^+]_i$, the sodium influx is augmenting the local Na^+ concentration to yet a higher level. These observations also seem consistent with earlier studies of the Na^+ sensitivity of cloned Slack channels in inside-out patches, which showed that there is a steep and accelerating relation between Slack channel activity and $[Na^+]_i$ (11). That study showed that raising $[Na^+]_i$ from 10 to 30 mM, increased Slack channel activity by only 20%, but raising $[Na^+]_i$ from 30 to 50 mM resulted in increasing channel activity by 70%. In the neurons we were studying, we asked the question: how high does the concentration of Na^+ reach in the local region sensed by Slack channels? To explore this question we loaded neurons with increasing concentrations of internal Na^+ by including Na^+ in the internal pipette solution. We found that, as long as the driving force on Na^+ was inward, we still could detect a TTX-sensitive delayed outward current, until we reached approximately 70 mM in the internal pipette solution. This suggests that the TTX-sensitive persistent Na^+ flux could still significantly

increase the local concentration of Na^+ in the vicinity of Na^+-activated K^+ channels, until the bulk intracellular [Na^+] approaches 70 mM. This, however, could be an underestimate since loading cells with high intracellular concentrations of Na^+ causes a substantial block of most K^+ channels (26).

Discussion

Na^+-activated K^+ channels are difficult to study because their activity is influenced by many factors including their Na^+-sensitivity, weak voltage sensitivity, channel run-down, modulation by second messenger systems, and, not the least, the mechanism and kinetics of Na^+ delivery to the channels themselves. Nevertheless, although the precise mechanism responsible for the local rise of [Na^+] is not fully established, our data strongly suggest that Na^+ entry through TTX-sensitive Na^+ channels, most likely carrying a persistent Na^+ current, activates a Na^+-dependent delayed outward current that is a large component of outward conductance in some neurons under normal physiological conditions. This result further suggests a very special relationship between Na^+-activated K^+ channels and TTX-sensitive sodium channels. Even at relatively high internal bulk concentrations of Na^+, e.g. 40 mM, an inward Na^+ current can still activate a substantial incremental component of delayed outward current. Thus, sodium entry appears to raise the local $[Na^+]_i$ affecting Slack channel activation to a level higher than that of the internal bulk solution. Although a diffusion barrier model might permit a local increase in Na^+, the electrostatic microdomain model might explain not only a local rise in [Na^+] but a unique requirement for persistent sodium entry as well. A putative electrostatic microdomain would most likely be non-selective and elevate both K^+ and Na^+ in relative proportion to their bulk intracellular concentrations. However, closely related persistent Na^+ entry might displace a significant amount of K^+, elevating the local [Na^+] to a higher level. Notably, Slack (SLO2.2) channels are similar to SLO1 channels in having a double ring of negative charges surrounding the inner vestibule of the channel (24). They also have other cytoplasmic domains with high net negativity, but the relevance of these features, if at all, to the mechanism of Na^+ -dependent gating of Slack channels must await further studies. Regardless of the exact nature of the Na^+-rich microdomain, our results suggest that Na^+ is normally maintained in it at a higher concentration than that of the bulk cytoplasm. TTX-dependent persistent Na^+ entry appears to occur over a wide range of voltages and there appears to be sufficient entry of Na^+ at a holding potential of −70 mV such that neurons maintained at that holding potential for long periods still exhibit a TTX-sensitive component of outward current even when test steps are taken to the Na^+ reversal potential. Thus, the possibility of a small contribution of persistent inward Na^+ current operating continuously at cell resting potentials and maintaining the local intracellular concentration of Na^+ higher than that of the bulk cytoplasm at the resting state cannot be excluded.

The potential role of the sodium channel-Na^+-activated K^+ channel coupled channel system may differ widely in different neuronal cell types, but in some, its impact may be profound. The relative contribution of the sodium-dependent delayed outward current relative to total outward current may increase as membrane resting potential becomes more positive because some voltage-dependent K^+ currents inactivate [e.g. A-type currents (27)], while Na^+-activated K^+ currents, and persistent sodium currents do not. These findings of a major but

previously unseen K^+ conductance have far reaching implications for many aspects of systems and cellular neuroscience, as well as clinical neurology and pharmacology. In systems and cellular neuroscience, studies of “up-down” states of neuronal excitability, spike adaptation, synaptic integration, and other aspects of neuronal physiology may have to be reexamined taking into consideration this system. In clinical and pharmacological studies, this previously unseen current system active during normal physiology represents a new and promising pharmacological target for drugs dealing with seizure and psychotropic disorders.

Methods

Dissociated MSNs were cultured from postnatal P2 rat pups, and recorded from 4–7 days post-plating. Recording solutions utilized an internal (pipette) [Na^+] as indicated in figure legends, and an external (bath) [Na^+] of 150 mM, or as indicated in figure legends. Experiments requiring the removal of external Na^+ replaced sodium with choline in the extracellular solution. Experiments which elevated Na^+ in the internal pipette solution removed equimolar K^+. Composition of recording solutions (in mM): *150 Na^+Bath Solution* (NaCl 150, KCl 5, $MgCl_2$ 2, Dextrose 10, HEPES 10, pH 7.4 with NaOH); *0 Na^+Bath Solution* (CholineCl 150, KCl 5, $MgCl_2$ 2, Dextrose 10, HEPES 10, pH 7.4 with KOH). Data were acquired using an Axopatch 200A or Axopatch 200B amplifier (Molecular Devices), digitized at 10 kHz using a Digidata 1440A (Molecular Devices), filtered at 5 kHz and collected using pCLAMP 10. Recording pipettes had tip resistances of 3–6 MΩ. In experiments using TTX or riluzole, drugs were added to external solutions at concentrations of 1 and 20μM, respectively. Sodium-dependent potassium currents sometimes exhibit "rundown" in the whole cell or detached patch recording modes. We did see “rundown” during the initial phase of recording currents in some cells. However we applied test voltage steps over time, prior to the application of TTX, or other treatments, and only initiated experiments after test pulses produced delayed outward currents that were stable over time [In general, in instances where the magnitude of the current decreased during initial test pulses, the current stabilized within ∼2 min].

Statistical analysis

We performed statistical analyses using Kirkman, T.W. (1996) Statistics to Use. http://www.physics.csbsju.edu/stats/ software. For comparison between two groups, we used paired Student’s t tests for the same procedures before and after applied treatments.

Animal Welfare

It is the policy of Washington University Medical School that all research involving animals be conducted under humane conditions, with appropriate regard for animal welfare. Washington University Medical School is a registered research facility with the United States Department of Agriculture (USDA) and is committed to complying with the Guide for the Care and Use of Laboratory Animals (Department of Health and Human Services), the provisions of the Animal Welfare Act (USDA and all applicable federal and state laws and regulations. At Washington University Medical School an Animal Care Committee has been established to insure compliance with all applicable federal and state regulations for the purchase, transportation, housing and research use of animals. Washington University

Medical School has filed appropriate assurance of compliance with the Office for the Protection of Research Risks of the National Institutes of Health.

Supplementary Material

Refer to Web version on PubMed Central for supplementary material.

Acknowledgment

We thank T. Hoshi and M. Nonet for their kind suggestions regarding the manuscript, and F. Sigworth and L. Kaczmarek for the Slack-HEK cell line used in control experiments. We also thank S. Harmon for his kind technical help and C, Santi and A. Butler for helpful comments. This work was supported by U.S. National Institutes of Health grants R24 RR017342–01 and R01 GM067154–01A1.

References

1. Kameyama M, et al. Intracellular Na^+ activates a K^+ channel in mammalian cardiac cells. Nature. 1984; 309:354–356. [PubMed: 6328309]
2. Dryer SE, Fujii JT, Martin AR. A Na^+-activated K^+ current in cultured brain stem neurones from chicks. J. Physiol. 1989; 410:283–296. [PubMed: 2795480]
3. Egan TM, Dagan D, Kupper J, Levitan IB. Na^+-activated K^+ channels are widely distributed in rat CNS and in *Xenopus* oocytes. Brain Res. 1992; 584:319–321. [PubMed: 1515948]
4. Dryer SE. Na^+-activated K^+ channels and voltage-evoked ionic currents in brain stem and parasympathetic neurones of the chick. J. Physiol. 1991; 435:513–532. [PubMed: 1770447]
5. Koh DS, Jonas P, Vogel W. Na^+-activated K^+ channels localized in the nodal region of myelinated axons of *Xenopus*. J. Physiol. 1994; 479:183–197. [PubMed: 7799220]
6. Dryer SE. Na^+-activated K^+ channels: a new family of large-conductance ion channels. Trends Neurosci. 1994; 17:155–160. [PubMed: 7517595]
7. Bhattacharjee A, Kaczmarek LK. For K+ channels, Na^+ is the new Ca^{2+} . Trends Neurosci. 2005; 28:422–428. [PubMed: 15979166]
8. Wallen P, et al. Sodium-dependent potassium channels of a Slack-like subtype contribute to the slow afterhyperpolarization in lamprey spinal neurons. J Physiol. 2007; 585:75–90. [PubMed: 17884929]
9. Yang B, Desai R, Kaczmarek LK. Slack and Slick K_{Na} channels regulate the accuracy of timing of auditory neurons. J. Neurosci. 2007; 27:2617–2627. [PubMed: 17344399]
10. Egan TM, Dagan D, Kupper J, Levitan IB. Properties and rundown of sodium-activated potassium channels in rat olfactory bulb neurons. J. Neurosci. 1992; 12:1964–1976. [PubMed: 1578280]
11. Yuan A, et al. The sodium-activated potassium channel is encoded by a member of the *Slo* gene family. Neuron. 2003; 37:765–773. [PubMed: 12628167]
12. Bhattacharjee A, Gan L, Kaczmarek LK. Localization of the *Slack* potassium channel in the rat central nervous system. J. Comp. Neurol. 2002; 454:241–254. [PubMed: 12442315]
13. Berg AP, Sen N, Bayliss DA. TrpC3/C7 and Slo2.1 are molecular targets for metabotropic glutamate receptor signaling in rat striatal cholinergic interneurons. J. Neurosci. 2007; 27:8845–8856. [PubMed: 17699666]
14. Pei Y, Tuschl T. On the art of identifying effective and specific siRNAs. Nat. Methods. 2006; 3:670–676. [PubMed: 16929310]
15. Hebert T, Drapeau P, Pradier L, Dunn RJ. Block of the rat brain IIA sodium channel alpha subunit by the neuroprotective drug riluzole. Mol. Pharmacol. 1994; 45:1055–1060. [PubMed: 8190096]
16. Alzheimer C, Schwindt PC, Crill WE. Modal gating of Na^+ channels as a mechanism of persistent Na^+ current in pyramidal neurons from rat and cat sensorimotor cortex. J. Neurosci. 1993; 13:660–673. [PubMed: 8381170]

17. Taddese A, Bean BP. Subthreshold sodium current from rapidly inactivating sodium channels drives spontaneous firing of tuberomammillary neurons. Neuron. 2002; 33:587–600. [PubMed: 11856532]
18. Chao TI, Alzheimer C. Do neurons from rat neostriatum express both a TTX-sensitive and a TTX-insensitive slow Na^+ current? J. Neurophysiol. 1995; 74:934–941. [PubMed: 7500162]
19. Fakler B, Adelman JP. Control of K(Ca) channels by calcium nano/microdomains. Neuron. 2008; 59:873–881. [PubMed: 18817728]
20. Abriel H, Horisberger JD. Feedback inhibition of rat amiloride-sensitive epithelial sodium channels expressed in *Xenopus laevis* oocytes. J. Physiol. 1999; 516:31–43. [PubMed: 10066920]
21. Pohl P, Saparov SM, Antonenko YN. The size of the unstirred layer as a function of the solute diffusion coefficient. Biophys. J. 1998; 75:1403–1409. [PubMed: 9726941]
22. Barry WH. Is "fuzzy space" necessary for Ca^{2+} extrusion on the Na^+-Ca^{2+} exchanger in cardiac myocytes? J. Mol. Cell. Cardiol. 1993; 25:641–643. [PubMed: 8411189]
23. Carmeliet E. A fuzzy subsarcolemmal space for intracellular Na^+ in cardiac cells? Cardiovasc. Res. 1992; 26:433–442. [PubMed: 1332825]
24. Brelidze, Tinatin I.; Niu, Xiaowei; Magleby, Karl L. A ring of eight conserved negatively charged amino acids doubles the conductance of BK channels and prevents inward rectification PNAS. 2003; 100:9017–9022.
25. Nimigean CM, Chappie JS, Miller C. Electrostatic tuning of ion conductance in potassium channels. Biochemistry. 2003; 42(31):9263–9268. [PubMed: 12899612]
26. Bezanilla F, Armstrong CM. Negative Conductance Caused by Entry of Sodium and Cesium Ions into the Potassium Channels of Squid Axons. JGP. 1972; 60:588–608.
27. Connor JA, Stevens CF. Voltage clamp studies of a transient outward membrane current in gastropod neural somata. J. Physiol. 1971; 213:21–30. [PubMed: 5575340]

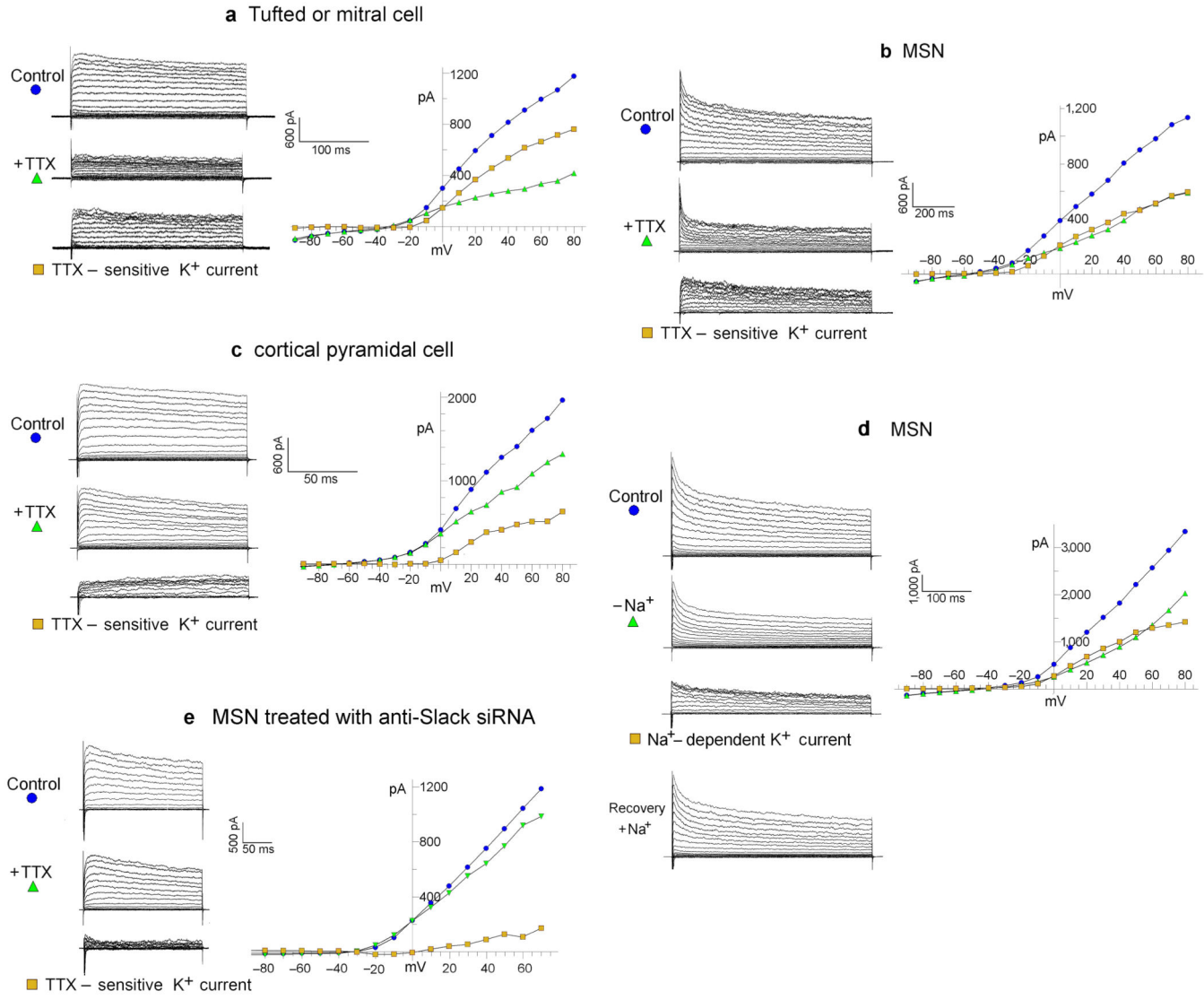

Figure 1. The TTX-sensitive (Na^+-dependent) delayed outward current, and its elimination by anti-Slack siRNA

(See Figure 2 for statistical analysis). **a, b, c**, The TTX-sensitive delayed outward current in tufted/mitral cell, MSN, and cortical pyramidal cell, respectively. Top traces show the family of control currents evoked from a holding potential of −70 mV. Middle traces show the outward current remaining after addition of TTX (1μM). Bottom traces show the TTX-sensitive current (TTX-sensitive K^+ current) which is the difference between the control currents before TTX, and the remaining currents after the addition of TTX. The current values shown in the I/V plots to the right were average values measured within the interval of 150 to 250 ms after the initiation of the voltage step. The intracellular pipette solution in these whole cell patch clamp experiments contained no Na^+. Also, Ca^{2+} was not present in the extracellular recording solutions. See text and Figure 2 for statistics. Some current traces in our experiments show unusual kinetics at the initiation of the voltage clamp step pulse. It is likely that these are anomalies due to the fact that TTX is not present, and therefore very

rapid inward Na^+ currents are opposing rapid transient outward currents at the initiation of the pulse, in a cell where the space clamp is not perfect (which is why TTX is so often used in studies of outward currents). **d**. The removal and subsequent replacement of extracellular Na^+ shows the Na^+-dependent delayed K^+ current in a MSN. **Control**: the family of control currents evoked from a holding potential of −70 mV. **−Na^+**: the outward current remaining after removal of external Na^+. **Na^+-dependent K^+ current**: the difference between the control currents before Na^+ removal and the remaining currents after Na^+ removal. **Recovery:** the current after reintroduction of extracellular Na^+ (see Figure 2 for statistics). The intracellular pipette solution in these whole cell patch clamp experiments contained no Na^+. **e**. An example of an MSN treated with Slack-siRNA having a smaller TTX-sensitive outward component. Experiments like these support the hypothesis that the TTX-sensitive delayed outward current is carried by Slack channels (See Figure 2 for statistics). Composition of recording solutions (in mM): *Bath Solution* (NaCl 150, KCl 5, $MgCl_2$ 2, Dextrose 10, HEPES 10, pH 7.4 with NaOH); *0 Na^+Bath Solution* (CholineCl 150, KCl 5, $MgCl_2$ 2, Dextrose 10, HEPES 10, pH 7.4 with KOH).; *Pipette Solution* (KCl 150, HEPES 10, EGTA 5, $CaCl_2$ 1, pH to 7.4 with KOH).

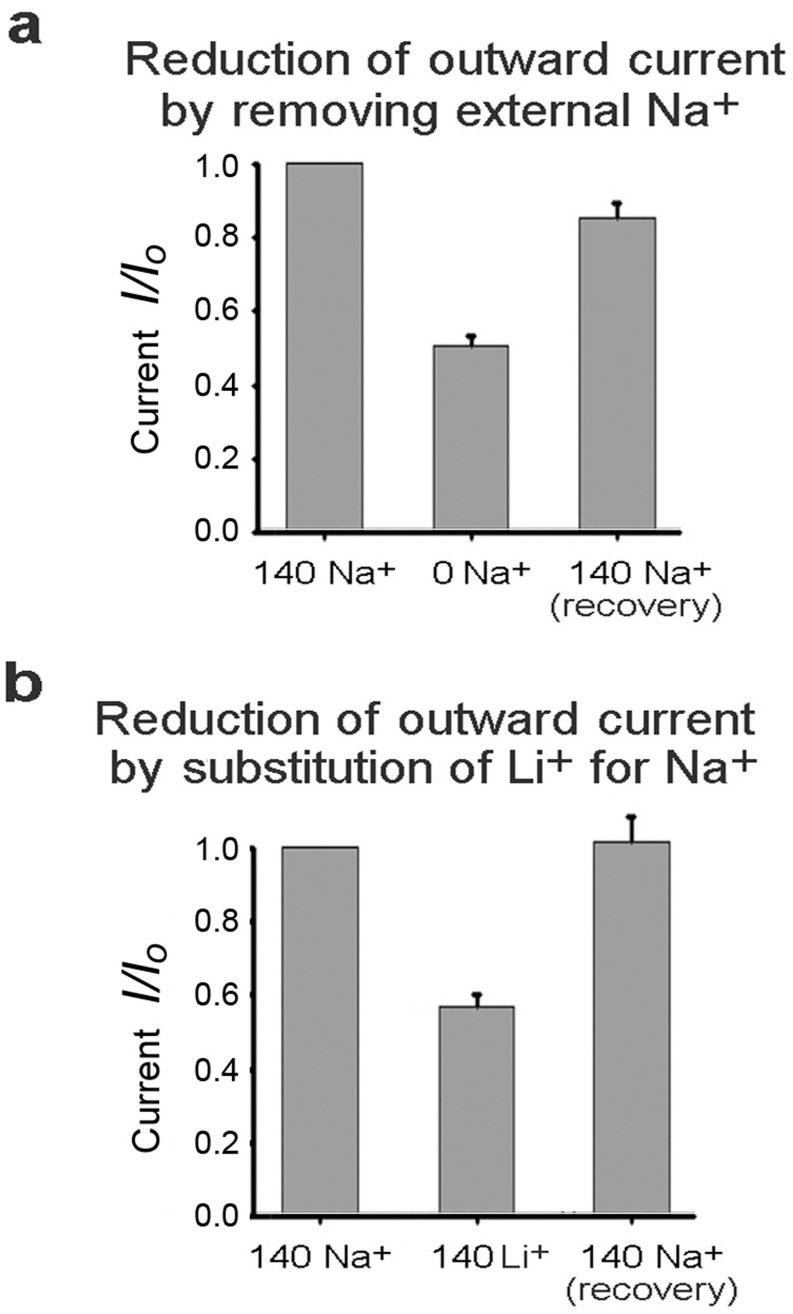

Figure 2. Inhibition of Na^+-dependent delayed outward current by a) the removal of extracellular Na^+ b) substitution of external Li^+ for Na^+

a. The removal of extracellular Na^+ reduced the delayed outward current by 49.9% +/− 2.3 % (n=8) *P*=<.01 in MSNs. Recovery after reintroduction of external Na^+ was 85.7% +/− 3.4% (n=7) *P*=.047 compared with starting control currents. This indicates that recovery after reintroduction of $[Na^+]_o$ may not have been quite complete. **b**. The substitution of external Li^+ for Na^+ reduced the delayed outward current by 41.6% +/− 3.1% (n=11)

P=<0.001. Recovery after reintroduction of external Na^+ was 103% +/− 8.0% (n=6) *P*=0.78 compared with starting control currents. Standard errors are shown.

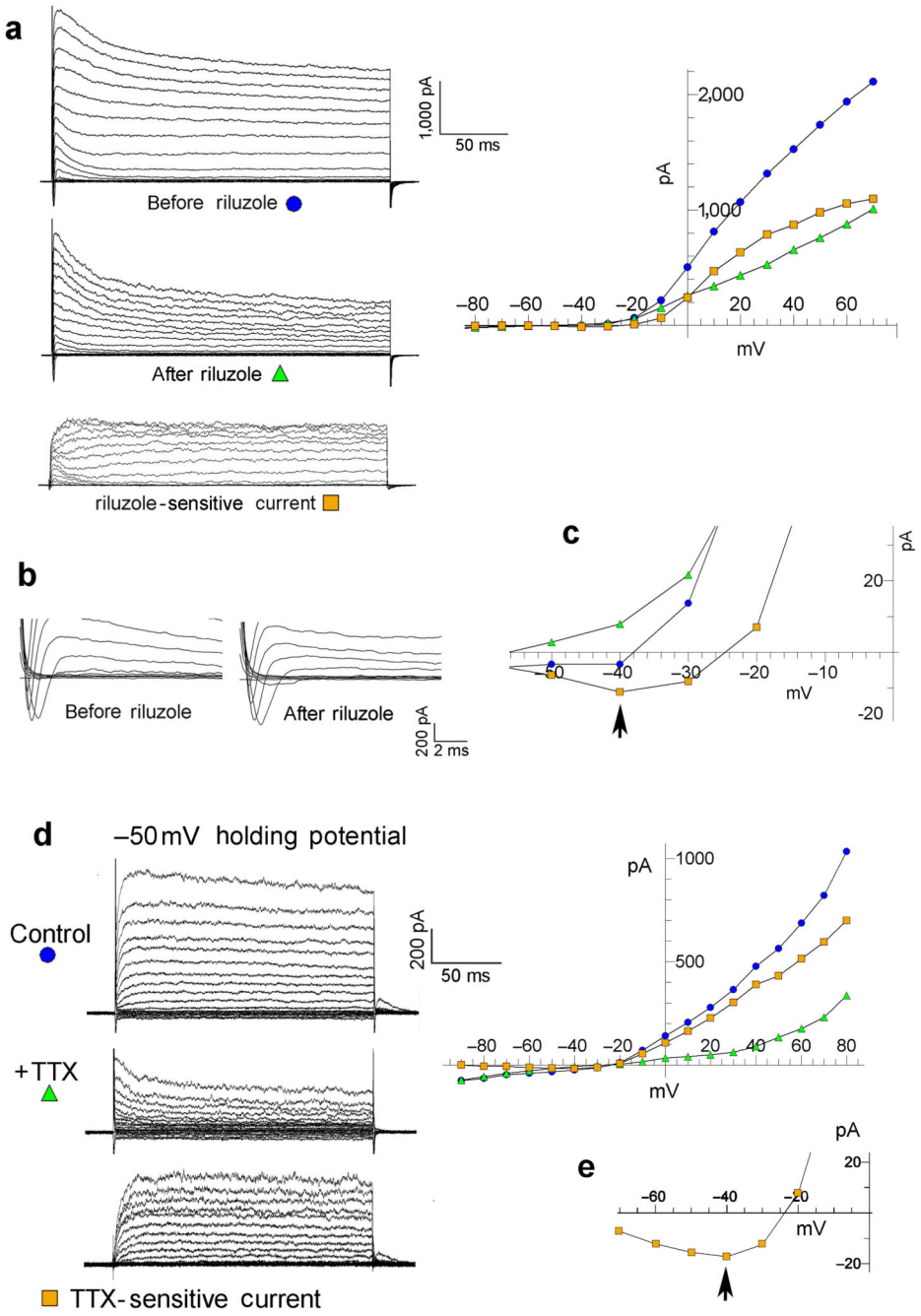

Figure 3. Evidence that a persistent Na^+ current activates the sodium-dependent delayed outward current

a–c Riluzole removes the persistent I_{Na}, but not the transient I_{Na}, and also removes a delayed outward current. **a**. Currents before and after the application of riluzole (20 μM) and the subtracted (Riluzole-sensitive) component recorded from a tufted-mitral neuron. The currents shown on the left are graphically plotted with respect to voltage on the right. Plotted currents were average amplitudes measured during the 150 –250 ms interval after initiation of the step pulse. **b**. Transient sodium currents in **a** at higher resolution showing no

reduction by riluzole. **c**. The base of the plotted current curves from the graph in **a** is shown at higher resolution. The arrow indicates a Riluzole-sensitive persistent inward current. Also note the TTX-sensitive persistent inward current in Figure 1e. [Note that in control experiments we did not find any block of Slack currents by recording delayed outward currents before and after applying riluzole (20 μM) to our stably Slack-transfected-HEK cell line. 20 μM riluzole added to the cell line resulted in a slight statistically insignificant increase in delayed outward current (4.83% +/− 3.02% n = 3). Currents were measured 200 msec after voltage step to +40 mV. The effect of riluzole was similar across all voltages tested (−90 mV to +80 mV).] **d**. The TTX-sensitive current shown from a holding potential of −50 mV. Except for the depolarized holding potentials other experimental details are as in Figure 1a. No transient inward sodium current was noted in this cell, yet the TTX-sensitive delayed outward current is well over half the total outward current. **e**. The base of the plotted current curves from the graph in **d** is shown at higher resolution. The arrow indicates a TTX-sensitive persistent inward current.

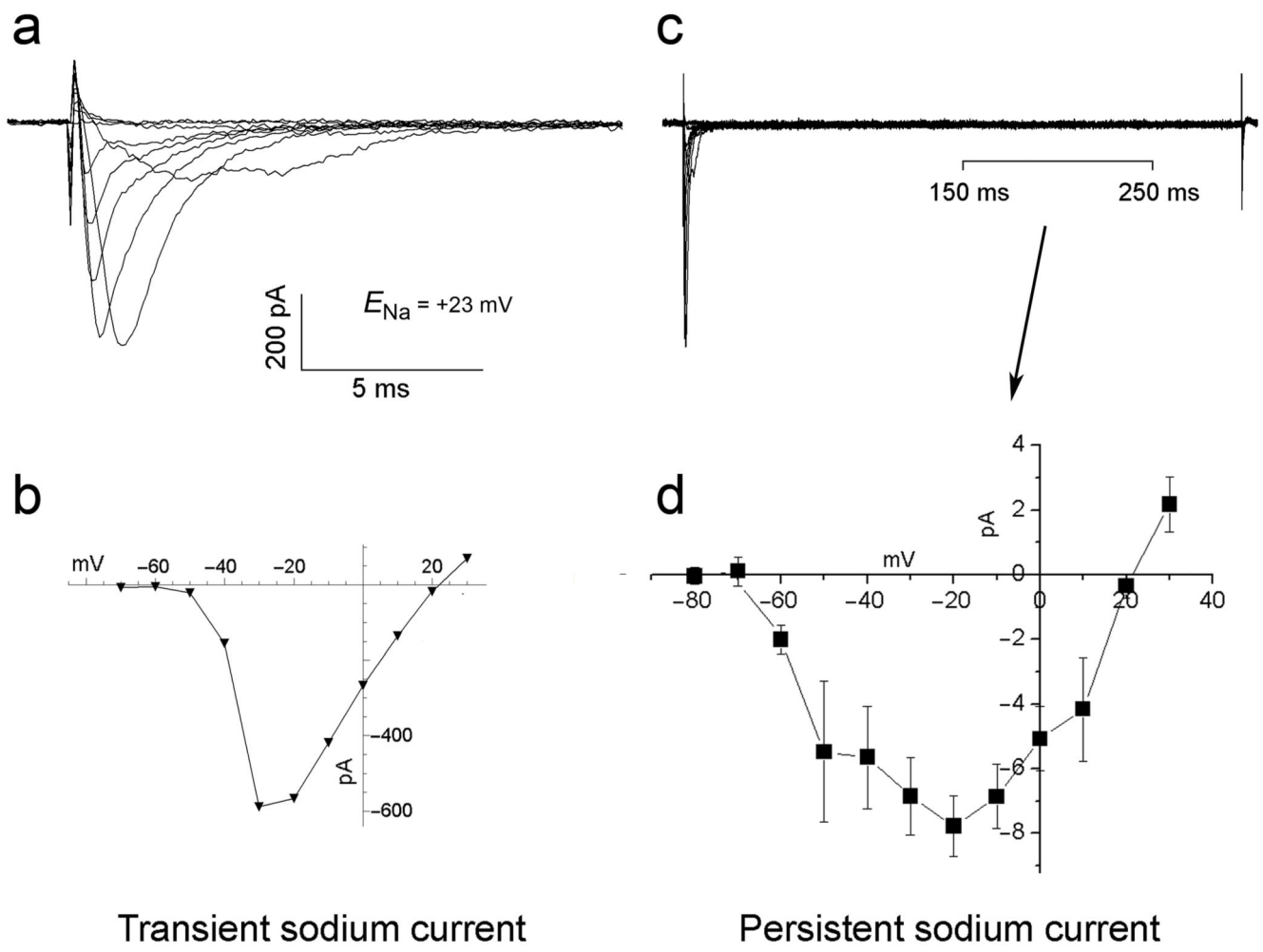

Figure 4. Transient and persistent Na^+ currents in MSNs

a,b Transient Na^+ current. **b,c** persistent inward Na^+ current. The persistent Na^+ current was plotted as the mean current during the 150–250 ms interval after the transient inward Na^+ current, as indicated in "**c**" (n=3). 100 mM cesium ion was used in the internal pipette solution and 40 mM TEA was used in the extracellular saline to block the potassium conductances. To isolate the TTX-sensitive components, we recorded currents before and after applying TTX; we then subtracted the residual currents after TTX from the currents recorded before TTX application. Thus, the currents shown represent both the TTX-sensitive transient and persistent components. The internal pipette solution contained 40 mM Na^+ to reduce the driving force of Na^+ and gain better voltage control. This also reduced the amplitudes of the currents. The approximate Na^+ equilibrium potential was +23 mV. Standard errors are shown.

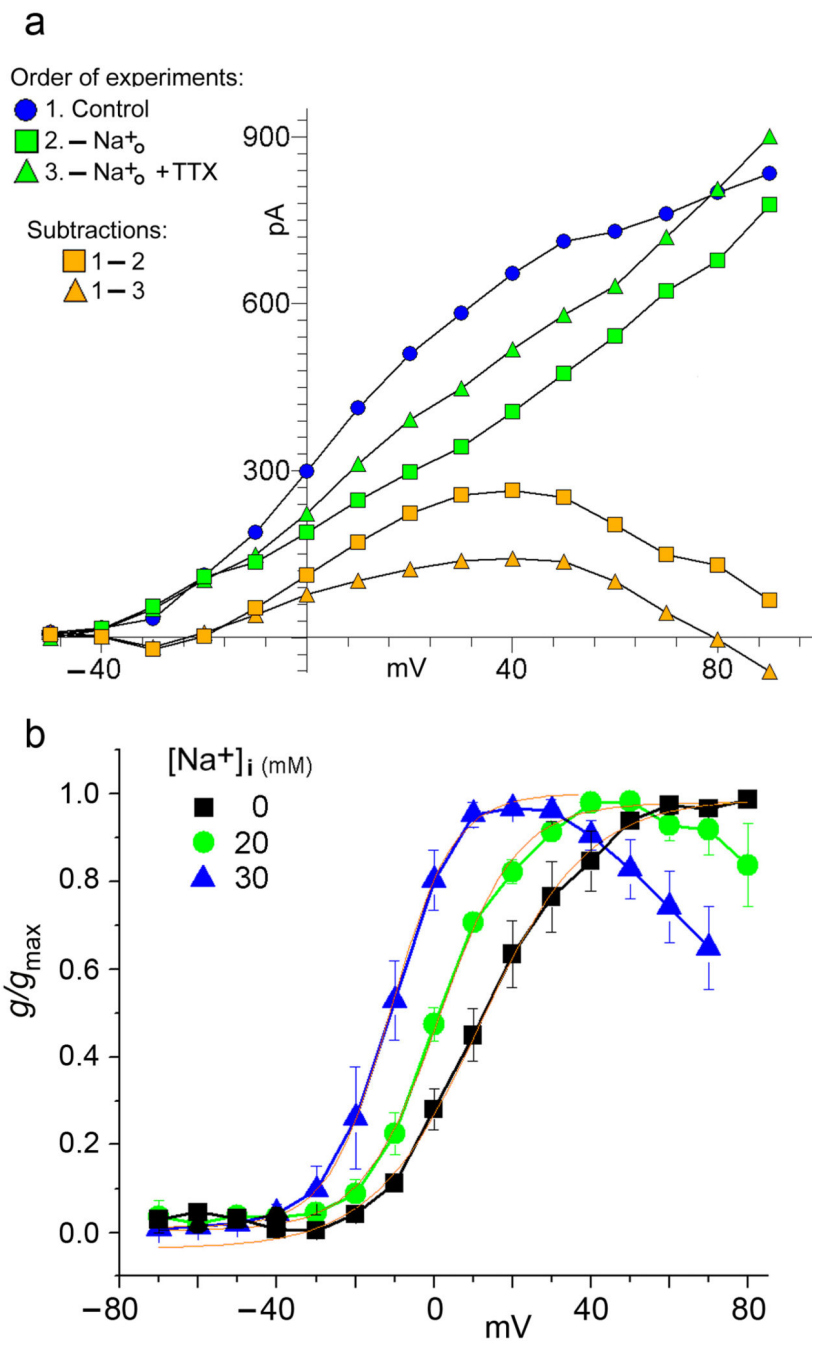

Figure 5. Experiments in cells loaded with high [Na^+]i

5a: inhibition of delayed outward current by sodium efflux from an MSN. Effects of reversing the direction of TTX-sensitive sodium flux across the membrane. The intracellular pipette solution contains 40 mM Na^+. **1. Control**: Delayed outward currents plotted from the cell with normal $[Na^+]_o$. A series of control voltage-clamp step pulses were applied at 10 mV intervals to a maximum of +90 mV. **2. -$[Na^+]_o$**: Outward currents plotted from the same cell after the removal of external Na^+. This plot shows the delayed outward current in response to the same series of voltage-clamp step pulses after reversing the direction of Na^+

current flow, which is now outward along the entire voltage range. **3. -$[Na^+]_o$ + TTX**: Outward currents plotted from the same cell after subsequently adding TTX to the 0$[Na^+]_o$ condition in 2. above. This plot shows the delayed outward current in response to the same series of voltage-clamp step pulses after reducing the outward movement of Na^+. Experiments shown in this figure were repeated seven times in MSNs and three times in tufted/mitral cells with similar results.

5b: Conductance/voltage relations showing the normalized incremental conductance increases in the delayed outward current due to Na^+ influx in cells loaded with different levels of $[Na^+]i$. Tufted/mitral cells "loaded" with different intracellular concentrations of Na^+, as indicated, were subjected to a series of voltage clamp step pulses. The incremental conductance/voltage curves plotted were constructed from the residual currents obtained by subtracting the currents recorded after removal of external Na^+, from the control currents recorded in normal $[Na^+]_o$ (as in Figure 5a, subtraction 1–2). As $[Na^+]i$ increases, the incremental conductance curves shift leftward to more negative voltages, and also show a steeper slope. This seems consistent with the hypothesis that, at higher concentrations of bulk $[Na^+]i$, the sodium influx is augmenting the local Na^+ concentration to yet a higher level. Conductances were calculated for individual cells at the three indicated concentrations, normalized to the maximum value, and then averaged. Regions of the curves to the left of Gmax were fit by a Boltzmann equation, shown in red. 0 mM $[Na]_{int}$ (■) $V_{½}$ = 11.8 mV, n = 3; 20 mM $[Na]_{int}$ (●) $V_{½}$ = 1.40 mV, E_{Na} = 50.8 mV, n = 3. 30 mM $[Na]_{int}$ (▲) $V_{½}$ = −11.0 mV, E_{Na} = 40.5 mV, n = 4.